ELSEVIER

Polymer 42 (2001) 1849–1861

polymer

www.elsevier.nl/locate/polymer

Synthesis, characterization and biodegradability of the biodegradable aliphatic–aromatic random copolyesters

H.C. Ki, O. Ok Park*

Department of Chemical Engineering, Korea Advanced Institute of Science and Technology, 373-1 Kusung-Dong, Yusong-ku, Taejon 305 701, South Korea

Received 4 January 2000; received in revised form 15 March 2000; accepted 5 July 2000

Abstract

Two series of biodegradable aliphatic–aromatic random copolyesters (PBCSTs) were synthesized by polycondensation. Specifically, we controlled the molar ratio of diols (1.4-butane diol, 1.4-cyclohexane dimethanol:CHDM) as well as that of diacids (succinic acid, dimethyl terephthalate:DMT) in order to investigate both the degradation behavior and the light transparency improvement of the final products. According to DSC observation, the melting temperature decreased gradually as more CHDM was added, and no melting temperature was observed when more than 20% of CHDM was used. Using 500 Mhz ^{1}H NMR, we noticed that succinic acid has the same reactivity as DMT. However, in diols, the composition of CHDM was richer than its feed. We also observed that the introduction of CHDM improved the transparency of the samples even though it deteriorated the mechanical properties slightly. In the hydrolytic degradation, the S70 series samples of which have more succinic units in their main chain, showed better degradability than S50 series samples at pH 10 and pH 7. Furthermore, S70C40 and S50C40 which contain much CHDM showed faster hydrolytic degradation than other samples because of their rich amorphous phase. In the composting experiment, in all samples, we found stains, which were the trace of growing microorganisms, on the their surfaces. Even S50C20 samples, which showed the lowest weight loss, showed severe surface degradation by the attack of microorganisms. Using simple empirical degradation models, we evaluated the effect of the crystallinity and the hydrophilicity. © 2000 Elsevier Science Ltd. All rights reserved.

Keywords: Aliphatic; Aromatic; Biodegradability

1. Introduction

In the world today, increasing volumes of plastics are manufactured and used for various applications because of their versatility and ability to be mass-produced. However, they usually are not naturally decomposing, and they are considered to cause some environmental problems. For this reason, many scientists have worked to develop new biodegradable polymers; some of these biodegradable polymers have been commercialized. However, the high price and weak properties of these polymers prevent them from being used in diverse applications. Blending and copolymerization techniques have been tried to obtain biodegradable polymers with improved properties [1–4]. Modified starch was blended with low-density polyethylene as a substitute for nonbiodegradable packaging films. Poly(hydroxybutyrate) PHB and poly(lactic acid) (PLA) were also blended with commercial polymers to cover their mechanical weaknesses. The blend of two or more polyester components can be changed into either block or random copolyesters depending upon the degree of the transesterification reaction at an elevated temperature in the presence of an adequate catalyst [5]. Using this method, the segment of biodegradable polyesters can be introduced into nonbiodegradable polyesters, and the average sequence length of each unit can be controlled. Some research has shown that these aromatic polyesters can be degraded when they are copolymerized with aliphatic polyester [6]. Even though the complete biodegradation of the aliphatic–aromatic copolyester is difficult since aromatic polyesters (e.g. poly(butylene terephthalate)) are usually resistant against microbial attack [7,8].

However, both blending and copolymerization methods still have some problems. In case of physical blending, only the biodegradable polymer portion can be attacked by microorganisms so that the nondegradable polymer portion will remain as in its original state after biodegradation. The copolymerization by transesterification seems to be uneconomical because of its multi-step process. To overcome these defects in aliphatic/aromatic polymer blends, their direct copolymerization methods are being investigated.

---

* Corresponding author. Tel.: +82-42-869-3923; fax: +82-42-869-3910.
E-mail address: oopark@cais.kaist.ac.kr (O. Ok Park).

PII: S0032-3861(00)00466-3

The biodegradability of polymers is influenced not only by the chemical structure of the polymers, especially the presence of functional groups and hydrophilicity–hydrophobicity balance, but also by the ordered structure such as crystallinity, orientation, and other morphological properties. The degree of crystallinity was known to be one of the major rate-determining factors of the biodegradability of polymers in the condition that the biodegradation starts in the amorphous regions and then continues into the crystalline regions.

In this study, we synthesized various aliphatic–aromatic random copolyesters, poly(butylene cyclohexanedimethylene succinate terephthalates) (PBCSTs), based on poly-(butylene succinate) (PBS) as a biodegradable aliphatic polyester with polycondensation method, controlling not only the diacid part(succinic acid, dimethyl terephthalate (DMT)) but also the diol part(1.4-butanediol (BD), 1.4-cyclohexane dimethanol (CHDM)). Then, we investigated the composition, thermal property and biodegradability of the copolyesters.

2. Experimental

2.1. Materials and Synthesis

For the diacid control, we used succinic acid(SA: Sinyo Pure Chem.) and DMT (Aldrich). Also, 1.4-BD (Junsei Chem.) and 1.4-CHDM (Aldrich) were chosen for the diol components control. Titanium tetraisopropoxide (TTI) which was purchased from Kanto Chem. was used as a catalyst. All materials were used without further purification for the polymerization. All copolyesters prepared in this work were synthesized employing the two-step polymerization method [9]. First, for the esterification, SA, DMT, BD and CHDM were placed into a four neck flask (1L) with the calculated molar diacid and diol ratios. TTI (0.5 wt% of monomer) was added to the flask. The flask, which was equipped with a stirrer and a condensation column, was submerged into an oil bath. The monomer mixture was melted at 180°C for 30 min. in the early stage. Then the temperature was raised to 200°C and maintained for 2 h 30 min in N_2 gas atmosphere. Second, polycondensation was carried out in a glass tube, which was placed in an oil bath. This glass tube reactor, which was equipped with a coil type agitator, was connected to a vacuum pump. The reaction was carried out at 270°C, and the pressure was reduced to 0.5 Torr for 3 h.

2.2. Measurements

Gel permeation chromatography (GPC) analysis was performed using a Waters 150C. Samples were dissolved in 0.1 Tetrahydrofuran (THF) (0.1 wt%) and filtered with a teflon filter(mesh size = 0.45 μm). The system was calibrated by polystyrene standards. To investigate the thermal properties of the prepared PBCSTs, DSC 2010 (Ta Instruments Inc.) was used. For the temperature sweeping experiments, heating and cooling rate were 10°C/min under the nitrogen atmosphere. The results of the second run were used for the investigation. The thermal stability of copolyesters was also investigated with a 951 thermogravimetric analyzer (Dupont Ins.). While samples were heated at a rate of 10°C/min up to 600° from room temperature, the weight loss of samples was monitored. Dumbbell type tensile samples were prepared using hot press (Carver) at the range from 100° to 160°C above their melting temperature. This test was followed by ASTM (D1708-96) with a universal tensile tester (Instron model 4201) at room temperature. The morphology of copolyester surfaces was observed with a Leica optical microscope. The cross-sections and surfaces of degraded samples after the hydrolytic degradation and the composting were also observed with a Philips 535 scanning electron microscopy (SEM). To observe the change of the polymer crystallinity during the hydrolytic degradation, X-ray diffraction (XRD) observation of the samples was carried out by a Rigaku X-ray generator. Sheet type samples that were prepared for the hydrolytic degradation test were used for this experiment. Also the samples that were used for the hydrolytic degradation experiment were collected and tested. For this experiment, the 2θ axis was scanned from 0 to 40°. Contact angle of copolyester surface with water was measured directly with Rame-Hart contact angle goniometer. Each reported contact angle is the mean of at least 8 independent measurements.

2.3. ^{1}H NMR characterization

To investigate the random copolymer composition and degree of randomness, ^{1}H NMR measurements were carried out using a Bruker AMX FR-NMR spectrometer operating at a resonance frequency of 500 MHz for protons. For the NMR spectra, the polymers were dissolved in $CDCl_3$(deuteriated chloroform) (2–5 wt%).

2.4. Hydrolytic degradation

Sheet type samples were prepared (initial film dimensions, 2 × 4 and 2–3 mm thick) with press molder and aged at least for 2 weeks at ambient temperature in order to let them reach a stabilized crystallinity before experiments. All samples were placed in vials containing aqueous buffer solutions at 30°C separately. PBS and PET samples were also used to compare the degradation rate. Three-type pH buffer solutions were used: pH 4, pH 7 and pH 10. Occasionally these buffer solutions were changed to maintain the constant pH conditions.

2.5. Biodegradation under aerobic composting conditions

The biodegradability test by composting in laboratory scale was executed on the basis of ASTM D6003-96, which is a standard test method for determining weight loss from plastic materials exposed to a simulated municipal

Table 1
Molecular weights of PBCSTs

	$\overline{M_n}$	$\overline{M_w}$	$\overline{M_z}$	PD
S50C00	26,300	46,800	70,700	1.78
S50C10	33,900	59,800	92,000	1.76
S50C20	32,200	63,900	102,500	1.90
S50C40	18,400	31,800	48,300	1.73
S70C00	17,800	34,200	56,400	1.92
S70C10	34,200	61,500	97,300	1.79
S70C20	28,300	44,400	64,100	1.56
S70C40	15,000	26,100	39,800	1.73

solid-waste (MSW) aerobic compost environment [10,11]. MSW consisted of 47% shredded leaves, 19.8% shredded news and computer paper (1:1 ratio), 2.5% saw dust, 10% meat waste (mixture of dog and cat food in a ratio of 1:1), and 20% soy bean. This mixture has a C/N ratio of 30–40. The air line was connected sequentially using tygon tubing, glass tubes, and rubber stoppers. Desired flow rates were maintained by flow meters and needle valves which were placed in line for each test vessel. The air that was used to provide oxygen to the bioreactors was humidified by passage through a 500 ml Erlenmeyer flask containing 350 ml distilled water. The air flow rate for each line was controlled at 80–90 ml/min by checking out the flow rate daily. The bioreactor was incubated in a temperature-controlled chamber. The temperature was set at 35°C for the first day and 55°C for the rest of the days. The moisture content was controlled to be 60% and the pH of the compost was 6.9. The test specimens were prepared as $22.5 \times 22.5 \times 2$ mm sheets. The biodegradation rate was determined by the weight loss (mg/cm^2) that was divided by the surface area of the initial sheet.

2.6. Sample identification

"S" in the sample code is used for succinic acid and "C" is for CHDM. The numbers at the end of each initial denote their initial feed mole fractions (%) of either total diol or total diacid monomer. For example, S70C20 represents a random copolyester synthesized with 70% succinic acid, 30% DMT, 80% BD, and 20% CHDM monomer, respectively.

Table 2
Thermal properties of the copolyesters (DSC:TGA)

	T_m	T_g	T_d	T_c	ΔH_f
S70C00	83.7	−22.3	366.6	29.8	35.5
S70C10	72.6	−21.5	372.5	*	1.6
S70C20	*	−11.4	377.6	*	*
S70C40	*	−1.3	381.3	*	*
S50C00	132.8	−8.9	371.3	*	21.8
S50C10	113.2	−3.1	376.4	54.4	14.8
S50C20	*	4.5	378.2	*	*
S50C40	*	18.4	382.0	*	*

3. Results and discussion

3.1. Thermal properties

The number average molecular weight of copolyesters was in the range of 15,000–34,000, and their polydispersity was 1.5–1.92 which is general in condensation polymerization (Table 1). At first glance, when we compare S50C00 with S50C10 and S70C00 with S70C10, we can notice that there is an increase in the number average molecular weight ($\overline{M_n}$). This result may imply that the apparent reactivity of CHDM is higher than BD. However, as more CHDM is added, lower $\overline{M_n}$ is observed both in the S50 series and in the S70 series. This result may indicate that, as the ratio of CHDM increases, the low volatility of the bulky cyclic structure of CHDM prohibits its extraction from the polymeric-melt. Therefore, this inhibits the further polymerization during the given polycondensation reaction time.

The thermal properties of the random copolyesters were measured using DSC and TGA (Table 2). In the DSC experiment, all samples were heated well beyond the melting temperature and cooled back to −50°C before the second run test. In comparison with S70C00, S50C00 that contains more aromatic repeating units, shows higher melting temperature because of the thermal stability of the aromatic substituents in the DMT unit. Both in the S70 series and in the S50 series, no melting temperature is observed in those samples in which the feed ratio of CHDM exceeds 20% by the molar diol base by the result of the CHDM effect on the crystallization. It indicates the severe disruption in crystalline structures, which arises from the *cis* and *trans* structures of the CHDM unit, and this crystalline disruption was more profound in the S70 series than in the S50 series. The heat of fusion (ΔH_f) data is consistent with these results. The reduction of heat of fusion of the S70 series is much more severe than the S50 series. The reason for this is that the aromatic repeating unit of DMT is more rigid than the aliphatic repeating unit of SA thus making somewhat easier maintenance of the polymer crystalline structure when the CHDM substituent attacks. However, thermally stable CHDM unit enhances the glass transition temperature (T_g). It is worth studying the thermal stability of the synthesized copolymers to investigate the effect of aromatic and cyclic units on thermal resistance of PBCSTs. The thermal degradation temperatures (T_d) which are estimated by thermogravimetric curves show that these PBCSTs have relatively better thermal stability than general aliphatic polyesters like PCL, PBS (Table 2). When we compare with S70C00, S50C00 has a higher thermal degradation temperature, because of the richer aromatic component in its main chain. As we already expected through the T_g behavior in the DSC results, the thermal degradation temperature is enhanced as feed CHDM ratio increases. So, we can conclude that both aromatic unit and cyclic unit enhance the thermal stability of these random copolyesters.

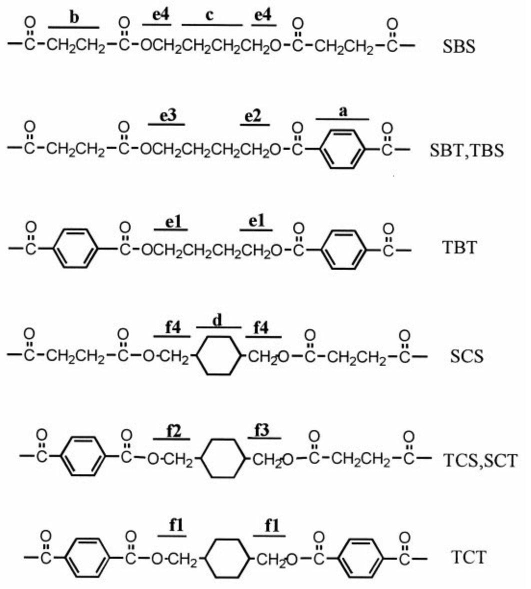

Fig. 1. All probable triad structures of the PBCSTs.

3.2. Polymer composition

To observe the reaction behavior, the composition of the samples was investigated using ^{1}H NMR. All probable structures of the reaction are shown in Fig. 1, and their coincident characteristic peaks were assigned (Figs. 2 and 4). In addition to that, each copolyseter composition was calculated by the area ratio of the each characteristic peak [12].

In the analysis of the diacids, 70% SA in the total diacid unit was included in the S70 series and 50% SA was included in the S50 series with no influence of increasing the CHDM. This result indicates that the reactivity of both SA and DMT is the same (Fig. 3(a)). However, in the analysis of the diol composition of the PBCSTs, we found that the ratio of CHDM unit in the total diol unit is higher than its feed ratio. All series showed the same tendency as shown in Fig. 3(b). The reason may be that lower vapor pressure of the bulky CHDM makes its extraction slower than BD from the polymeric melt during the reaction, and it causes relatively higher reaction probability of the CHDM than BD. As CHDM feed increases, however, the relative density of total diols increases during the same reaction time so that the overall reaction is retarded. The change of the diol composition and the $\overline{M_n}$ of the S70C10 by changing the polycondensation reaction time show well this reaction phenomenon. The CHDM peak area of the NMR analysis was enlarged as the reaction time increased from 14.1% for 3 h to 15.2% for 4 h and the $\overline{M_n}$ was also increased from 34,000 to 48,000.

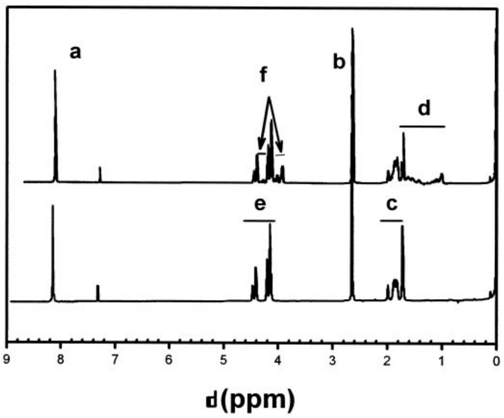

Fig. 2. The characteristic peaks of all probable structures. (500 MHz ^{1}H NMR).

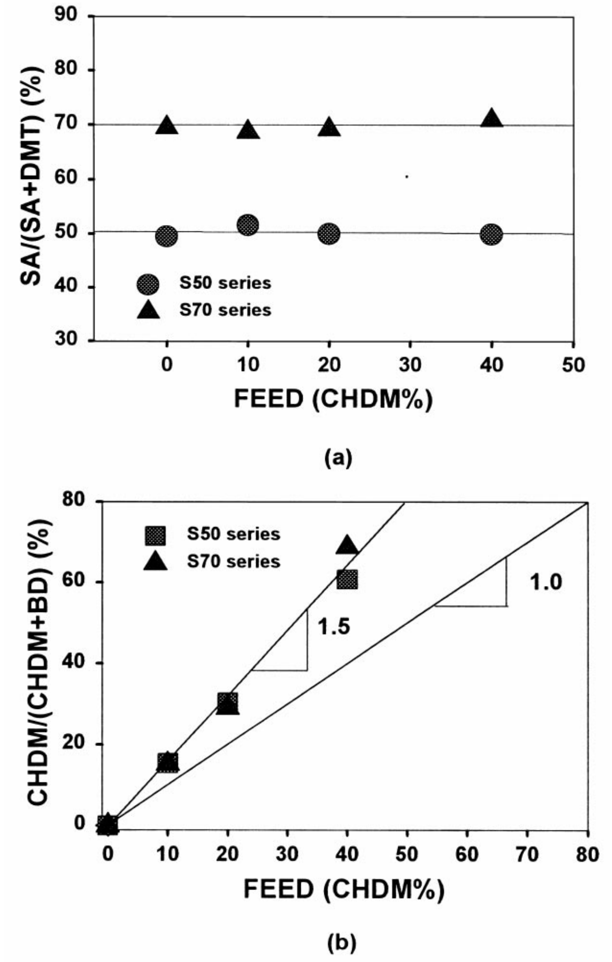

Fig. 3. Diacid, Diol composition in the PBCSTs. (a) SA content in the PBCSTs. (b) CHDM content in the PBCSTs.

In the polymer biodegradation, the monomer sequence distribution in the copolymer chain is very important to the understanding of whether microorganisms attack only aliphatic ester block of the blocked polymer chain or whether they can randomly attack well-distributed aliphatic–aromatic units. To investigate this monomeric sequence distribution in the copolymer chain, many scientists adopt the concept of the degree of randomness [13,14]. Using this concept, we tried to investigate the average sequence

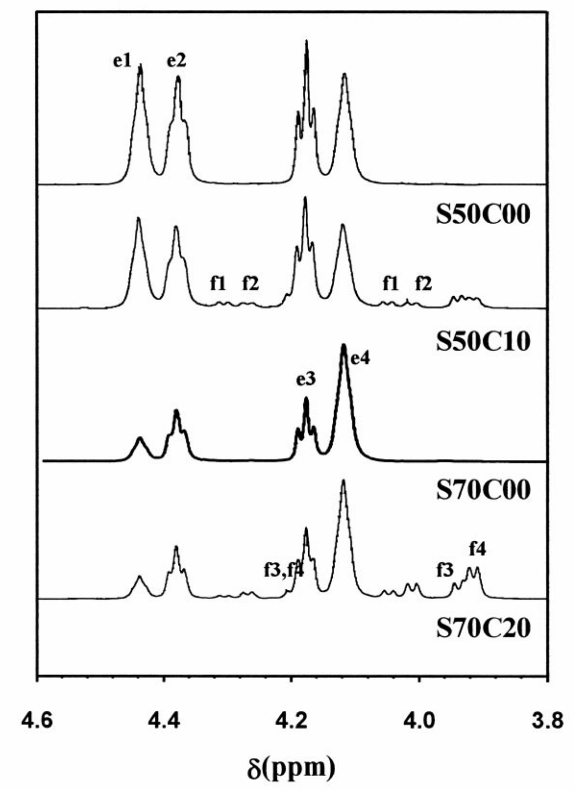

Fig. 4. The peak assignment of the methylene peak in diols.

distribution of the prepared PBCSTs using their triad sequence analysis. In the absence of the CHDM unit, the methylene substituent peaks in BD (c; 1.7–2.0 ppm, e;4.1–4.5 ppm) were used. But, when the CHDM was introduced, the chemical shift of CHDM unit (d; 0.9–2.9 ppm) severely overlapped with the methylene proton peaks of BD (c; 1.7–2.0 ppm). So the methylene proton peaks of CHDM(f; 3.9–4.3 ppm) and BD (e; 4.1–4.5 ppm) were used to analyze their sequence distribution characterization in the NMR spectrum. The assignment of each characteristic proton peak is shown in Fig. 4. The randomness of the each copolyester sample was confirmed by NMR data. The average length of repeating succinic acid units were about 3.2 in the S70 series and about 2.0 in the S50 series, which we can expect the higher possibility of the biodegradation in the S70 series than in the S50 series.

3.3. Mechanical properties and light transparency

Table 3 shows tensile modulus, strength, and elongation of the Instron tests, respectively. In both the S70 and the S50 series, the tensile modulus shows its decreasing behavior. One of the reasons is that the additional CHDM unit disrupts the polymer crystal which maintains its tensile strength by the attractive force between polar groups in it [15]. Therefore, the samples, which have low crystallinity, seem to show low tensile strength and modulus. As discussed before, the molecular weight decreases as the CHDM increases in each series. Therefore, we have to consider the effect of the molecular weight, which affects the tensile properties of the polymer. Therefore, the tensile properties in each series are lowered not only by the CHDM composition, but also by the molecular weight reduction of synthesized PBCSTs.

General biodegradable copolyesters that are synthesized by the polycondensation like PBS and PBA are highly opaque. To be used in a diverse application, these polyesters need to have light transparency. In this study, the crystallinity was controlled with controlling the ratio of the CHDM, and we obtained relatively clear copolyesters. In Fig. 5, S50C40 and S70C40 show high transparency, which indicates that these copolyesters are amorphous. Moreover, we can expect higher degradability because of the amorphous matrix of these copolyesters.

3.4. Contact angle of copolyester

Surface hydrophilicity of polymers is reported to be a factor affecting the degradation rate [16]. Its effect on the bacterial adhesion and protein adsorption trends has been observed at a high level on hydrolytic surfaces and compared with hydrophilic surfaces [17]. Fig. 6 shows the contact angle of water on the surface of each copolyester series. In this figure, the S50series shows a higher contact angle than the S70 series because of the more hydrophobic aromatic unit. Moreover, it increases sharply as the ratio of CHDM increases. This indicates both DMT and CHDM make the copolyester surface more hydrophobic. And, this information will be discussed deeply in regard to the hydrolytic degradation and composting biodegradation as a factor representing DMT and CHDM composition dependency.

Table 3
Tensile properties for the copolyesters

	Tensile modulus (MPa)	Tensile strength at yield (MPa)	Strain at yield (%)	Tensile strength at break (MPa)	Strain at break (%)
S50C00	97	12	29	20	680
S50C10	48	8	36	19	69
S50C20	28	6	43	20	720
S50C40	70	11	33	14	290
S70C00	176	13	15	19	460
S70C10	93	10	22	17	530
S70C20	235	6	26	7	130
S70C40	13	*	*	6	410

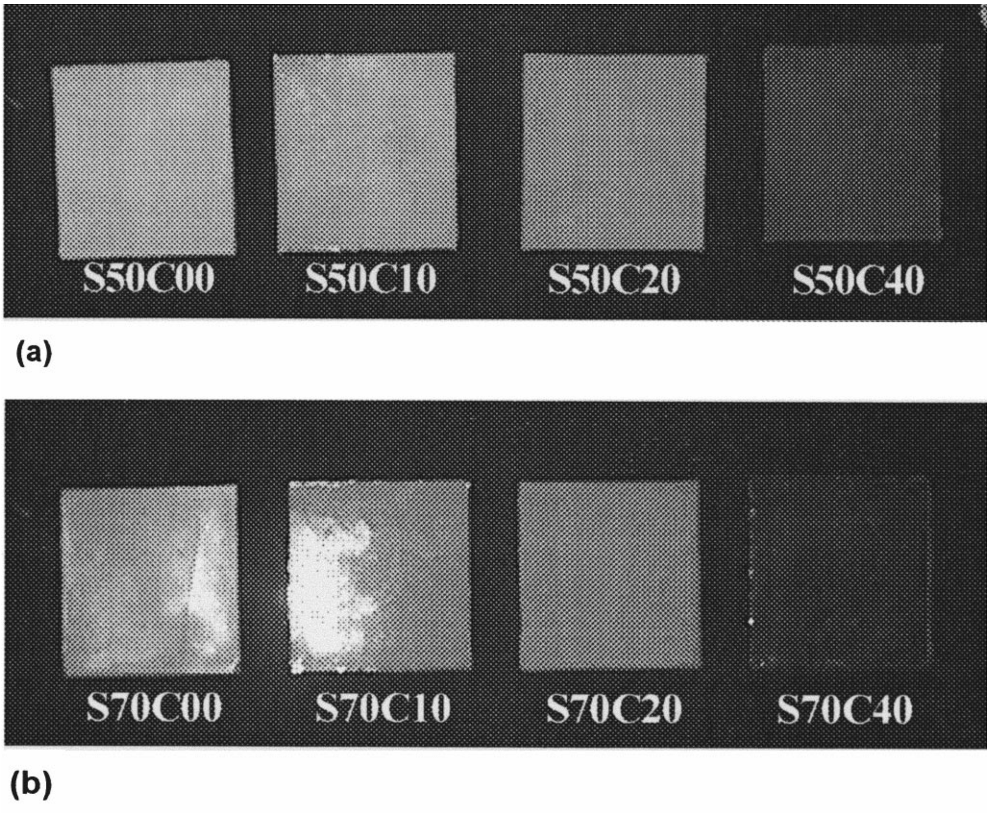

Fig. 5. Light transparency of the copolyester sheet. (a) S50 series. (b) S70 series.

3.5. Hydrolytic degradation

Degradation of aliphatic polyesters derived from the condensation polymerization of diols and dicarboxylic acids, in general, proceeds more or less by hydrolysis with or without the presence of an enzyme, depending on their chemical, configurational and morphological structures [18]. This hydrolytic degradation depends primarily on the kinetics of the chemical cleavage of an ester according to

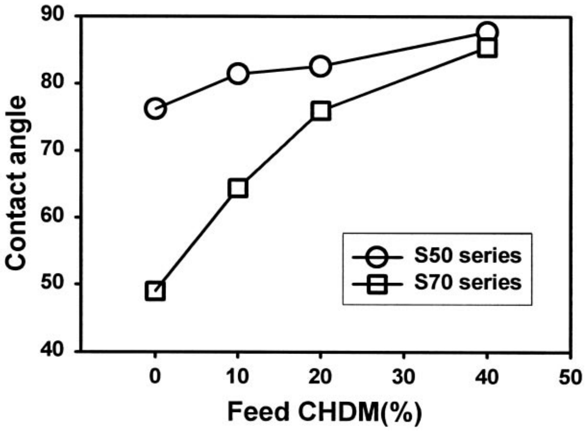

Fig. 6. Water contact angle of the PBCSTs.

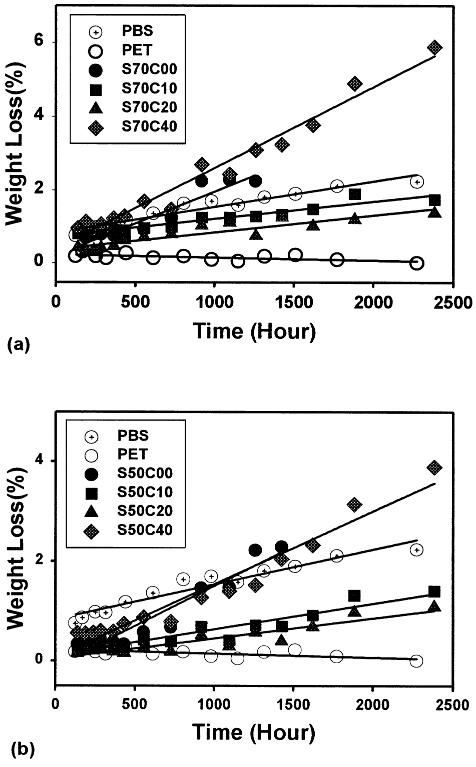

Fig. 7. Hydrolytic degradation and the empirical relations between time and weight loss at pH 10, 35°C. (a) S70 series. (b) S50 series.

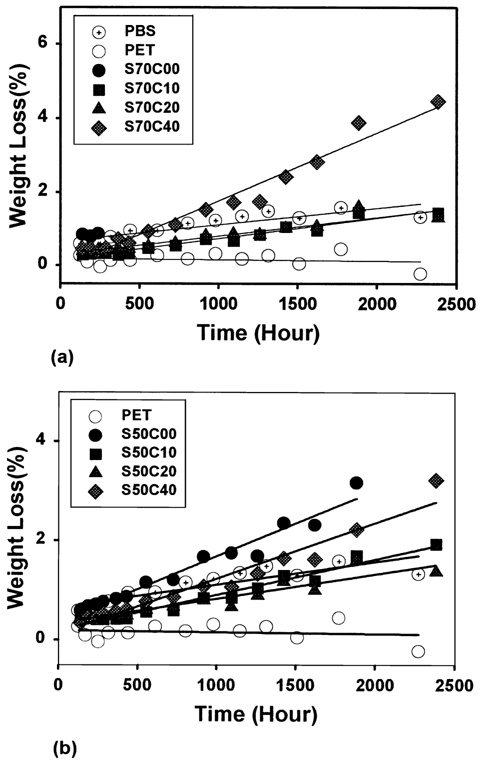

Fig. 8. Hydrolytic degradation and the empirical relations between time and weight loss at pH 7, 35°C. (a) S70 series. (b) S50 series.

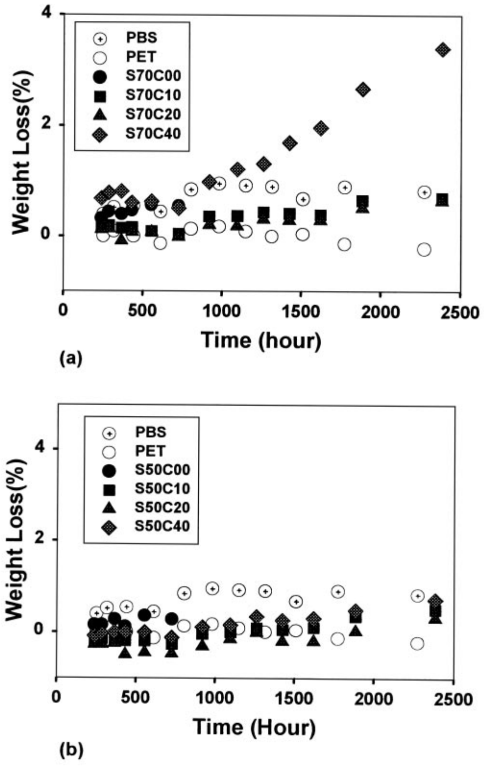

Fig. 9. Hydrolytic degradation and the empirical relations between time and weight loss at pH 4, 35°C, (a) S70 series. (b) S50 series.

the well-known reaction

$$\mathrm{R{-}COO{-}R' + H_2O \rightarrow RCOOH + R'OH}$$

In the hydrolytic degradation test of PBCSTs (including PBS, PET which were used as an affirmative and a negative reference sample, respectively), as shown in Figs. 7–9, we found that all samples degrade even though they have many aromatic units in their main chain and that some of the samples degrade faster than PBS. The fast degradation of aliphatic–aromatic random PBCSTs may come from the fact that these copolyesters have less crystallinity than PBS so that water permeation into each polymer is easier than PBS. In addition to that, the lower glass transition temperature of the samples than experimental temperature maintains the chain mobility [19]. The rate of degradation monitored in each series revealed DMT composition dependency. As presented in Fig. 7–9, the degradation rate of the S70 series is higher than the S50 series when compared with each sample which contains the same amount of CHDM. As we already expected, the longer average length of repeating succinic acid unit in the S70 series (LnS:3.2) makes the chain scission easier than the S50 series (LnS:2.2) during hydrolytic degradation. The rate of degradation also depends on the CHDM composition. The degradation rate is retarded with increasing CHDM content up to 20 mol% feed. Then, the degradation rate begins to rise in the sample which was fed 40 mol% CHDM in each series. So the presence of DMT and CHDM units may promote the hydrophobic nature of these copolyesters which would negatively influence the hydrolytic susceptibility by sterically hindering the access of nucleophiles. However, the introduction of these structures should render copolyester more amorphous and less resistant to nucleophilic attack.

Generally, we can find the polymer crystallinity by the group contribution concept [20] with the heat of fusion at DSC thermograms. However, in this case, it was very hard to use this method because of the difficulty in finding the CHDM contribution to any polymers. Therefore, XRD can be an appropriate method. In the S70 series, the peaks of the S70C00 at $2\theta = 21.33$, 21.94 and 22.60° decrease as the CHDM ratio increases, and the new peak at 16.95° is generated. In S 50 series, among the characteristic peaks at 16.36, 17.32, 23.20 and 24.88° of the S50C00, only two peaks at 16.36, 24.88° diminish severely. This result assists the previous result, which we discussed in the thermal properties, that the rigidity of the aromatic repeating units in a crystal somewhat maintains its structure more than the aliphatic repeating unit does when the CHDM substituent attacks.

In all series, the crystallinity of the copolyesters decreases as the CHDM unit increases, which we already expected in the DSC thermograms. Table 4 shows the crystallinity of the PBCSTs and its change after the hydrolytic degradation. In all samples, we can find that the crystallinity increases, even though the total weight loss of the samples was at most 6% in the hydrolytic degradation. So, there is a possibility that

Table 4
Crystallinity change after the hydrolytic degradation

Sample Code	Before the hydrolytic degradation (%)	After the hydrolytic degradation (%)
S50C00	39.7	53.8
S50C10	32.4	37.0
S50C20	22.4	33.8
S50C40	16.2	25.0
S70C00	43.2	46.0
S70C10	39.0	40.8
S70C20	26.7	32.6
S70C40	7.4	13.9

we can control the degradability by changing the polymer crystallinity.

Zimmerman and co-workers studied the hydrolytic degradation rate of polyesters [21], and more recently the effects of molecular weight and crystallinity in the hydrolytic degradation rate have been reported [22]. The hydrolytic degradation of polyesters involves the chemical scission of an ester linkage by a water molecule. Each chain scission uses one water molecule and creates one carboxyl end group. Hence, the reaction can be analyzed by measuring the number of carboxyl ends present after various hydrolytic degradation times. However, using this method, it is complicated to compare the effect of the crystallinity and the hydrophilicity in the long-term scale experiments in which we deal with the diverse composition. Therefore, in this study, we set an empirical model that the weight loss shows apparently linear dependency on time in the early stage of hydrolytic degradation. Moreover, by doing this, we could easily evaluate the crystallinity and the hydrophilicity effect on the hydrolytic degradation with the slope, as a reaction rate constant, in the time vs. weight loss plot.

Fig. 10(a) shows well the hydrolytic degradation behavior, in which the degradation reaction rate constant k decreases as the contact angle increases up to the first three points of each series. However, the introduction of the CHDM renders the copolyester more amorphous and less resistant to the nucleophilic attack as discussed previously. Hence, the reaction rate constant k rises again at the last points of each series. This effect of the crystallinity is shown in Fig. 10(b). We can apply this model to the pH 7, and the same behavior is observed.

In this hydrolytic degradation experiment, the weight loss of the all samples was faster under alkaline conditions than pH 7, and pH 4. It is because a base promotes hydrolysis of esters by providing the strongly nucleophilic reagent OH^-. Moreover this reaction is essentially irreversible since a resonance-stabilized carboxylate anion shows little tendency to react with an alcohol [23]. Figs. 7–9 show this behavior at different pH conditions.

In the pH 10 condition, we found many degradation-induced cracks on the surfaces of the S50C00, S70C00, S50C40, S70C40 and PBS samples that were not observed in other PBCSTs and in other pH conditions. These cracks show their higher degradation rate under the alkaline conditions. Fig. 11 shows the degradation inducing cracked morphologies of PBCST that were observed by an optical microscope. The morphology of each inner crack is also shown in Fig. 12 using SEM. In this figure, PBS and S70C00 show some narrow empty voids that are unlike other samples. Some of aliphatic polyesters (PLA, PGA) are reported to degrade faster in the internal region by autocatalysis [24]. By this reaction–diffusion process the polymer matrix is homogeneous in the sense that the average $\overline{M}_w$ is the same throughout the matrix. Once the specimen is placed in an aqueous medium, water penetrates into it leading to hydrolytic cleavage end group that, according to autocatalysis, accelerates the hydrolytic reaction of the remaining ester bonds. At the very beginning, degradation occurs in the bulk and is macroscopically homogeneous. However, the situation becomes totally different as time passes. Because soluble oligomers that are close to the surface can escape from the matrix before total degradation while those located inside the matrix can hardly diffuse out the matrix. This difference results in a higher acidity inside than at the surface. Likewise, some of these copolyesters show empty voids in the cross-section. This implies that there exists a diffusion balance between soluble oligomers and water in PBCSTs. In other words, DMT and CHDM, which prevent the access of water on the polymer surface, make more hydrolytic degradation occur at the polymer surface preferentially.

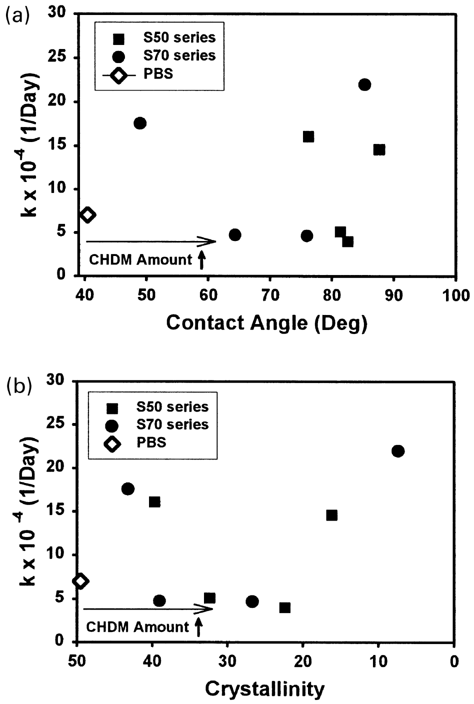

Fig. 10. The effect of the crystallinity and of the contact angle on the hydrolytic degradation, which is evaluated with k (pH 10). (a) Contact angle vs. k. (b) crystallinity vs. k.

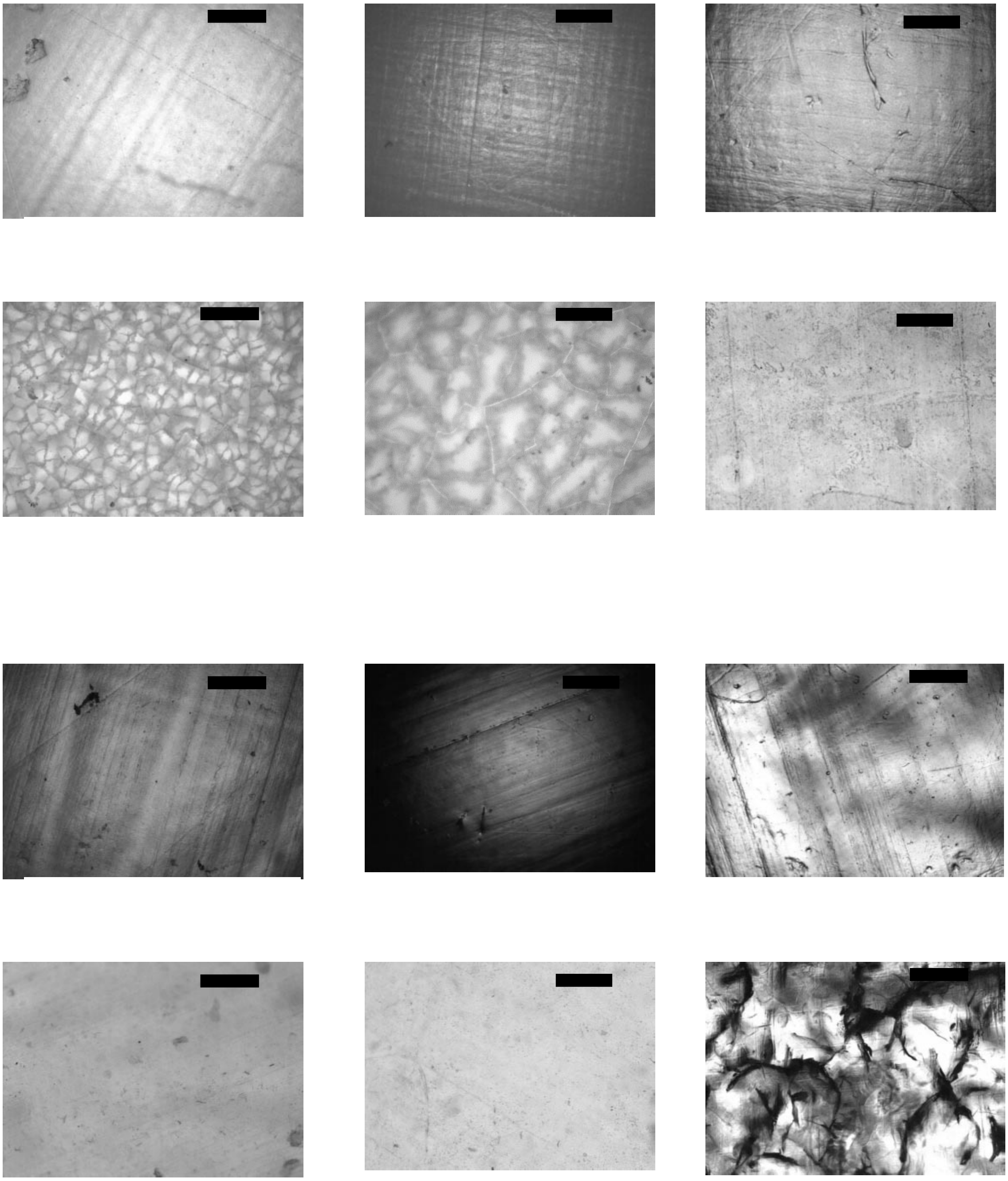

Fig. 11. Surface morphology of the copolyesters. (Observed with an optical microscope at pH 10, before and after the hydrolytic degradation).

3.6. Composting biodegradation

Biodegradable copolyesters containing aromatic units have been reported recently [25,26] and various microorganisms were investigated for these aliphatic–aromatic copolyesters [27]. It has been known that copolyesters containing adipic acid and terephthalic acid are attacked by microorganisms. A polyester derived from phthalic, isophthalic or terephthalic acid and poly(ethylene glycol) (PEG) is assimilated by symbiotic mixed cultures of a phthalate ester-hydrolyzing bacterium and a PEG-utilizing bacterium.

In this work, the biodegradability of PBCSTs was examined using the composting experiment. Composting is a good method to investigate the biodegradability of a polymer. The degradation process in compost also takes place in soil, so it can be considered to be synonymous with degradation in soil conditions, with the exception that degradation rates in composting are higher than in natural conditions because of the higher temperature. In this composting

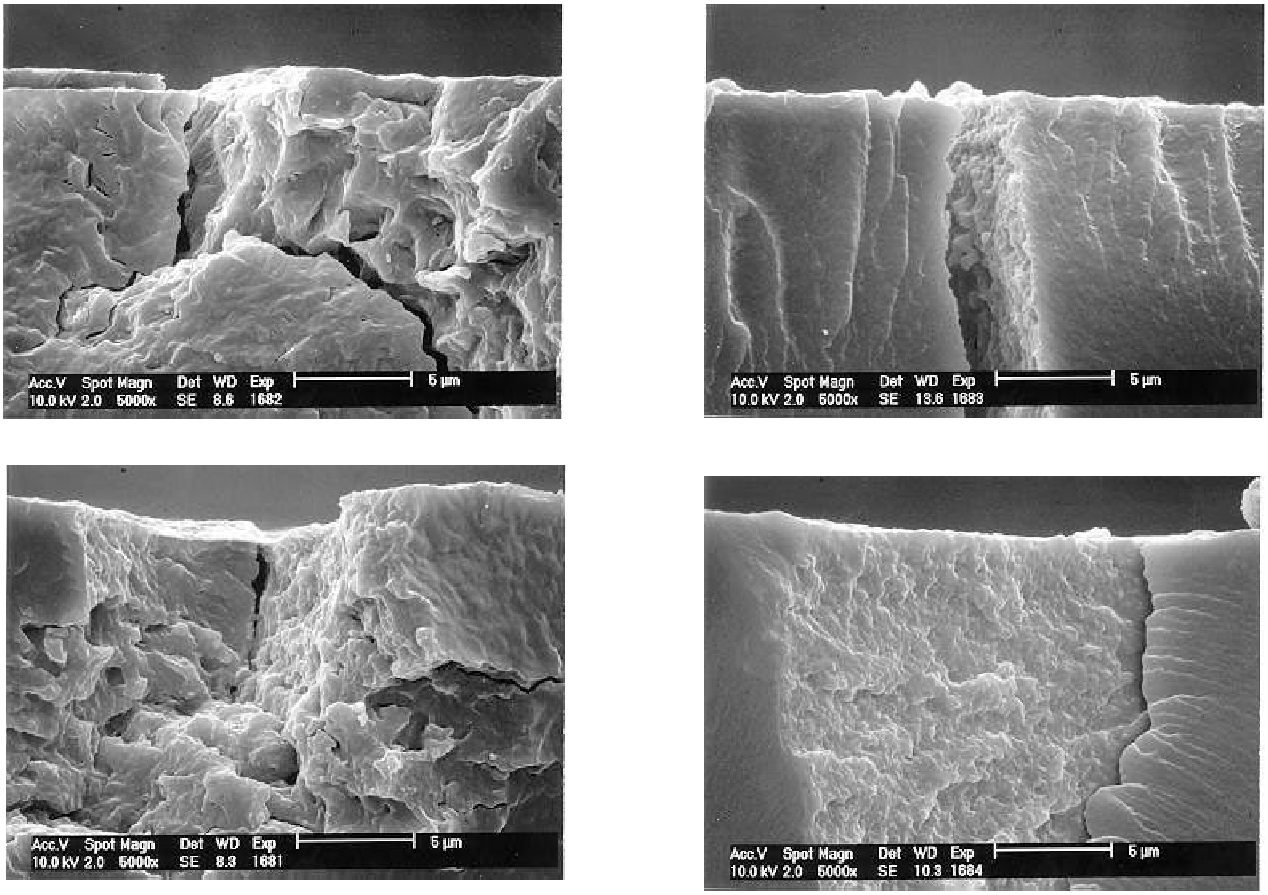

Fig. 12. The morphology of each inner crack (SEM).

experiment, poly(ethylene terephthalte) (PET) and PBS were also used as the reference materials to verify the validity of composting test. The weight losses of copolyesters and reference samples are shown in Fig. 13. As we have seen in the results of the hydrolytic degradation, the S70 series shows higher degradation rates than the S50 series.

For the same reason of the hydrolytic degradation, it can be useful to use the degradation rate constant in determining the effects of crystallinity and hydrophilicity of the biodegradation under the composting conditions. However, the mechanism of the biodegradation is quite different from the hydrolytic degradation, in the sense that the biodegradation arises on the surface of the polymer. And the number of microorganisms increases exponentially in an early stage of composting. To get a simple model which is represented by the weight loss of the polymer, it is reasonable to assume the polymer weight loss by the biodegradation follows exponential decay function.

Then we can get a simple reaction rate model that is represented by the weight loss of the samples

$$\frac{W}{W_0} = e^{-kt} \tag{1}$$

$W_0 =$ Initial weight of the sample

$$\frac{W_{\mathrm{Loss}}}{W_0} = 1 - e^{-kt} \tag{2}$$

where

$$W_{\mathrm{Loss}} = W_0 - W$$

Then

$$\frac{W_{\mathrm{Loss}}}{\mathrm{Area}} = b \cdot \rho (1 - e^{-kt}) \tag{3}$$

Here is the final model of the composting biodegradation with which we can simply compare the effects of crystallinity and hydrophilicity in the composting biodegradation of all samples with two parameters. Moreover, b is a constant that is expressed as the thickness of the sample, and we know the density of each sample. So, only k is the parameter that we will use. The density of each series is listed in Table 5, and the parameter k is obtained by the log plot of Eq. (3) (Fig. 14). The results are also plotted in Fig. 15. In this figure, we can instinctively investigate the effect of the crystallinity and the hydrophilicity as discussed in the hydrolytic degradation.

The k values of the S50 series show the same behavior as the hydrolytic degradation showed at pH 7, where the degradation rate is retarded with increasing CHDM content up to

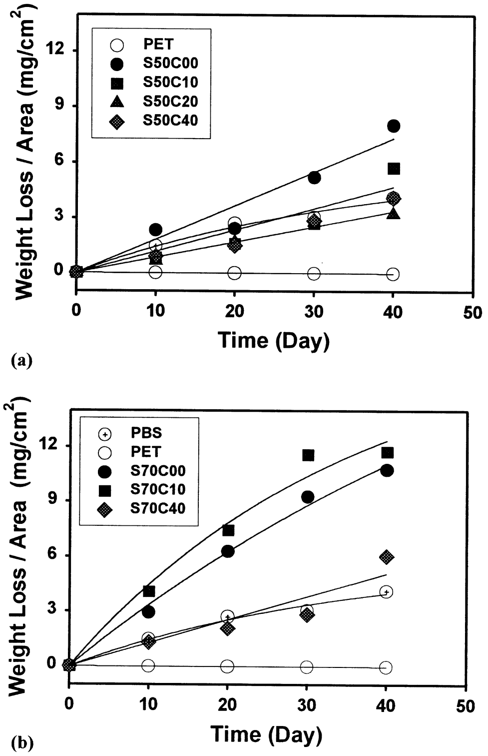

Fig. 13. Composting biodegradation. (Measured by weight loss). (a) S50 series. (b) S70 series.

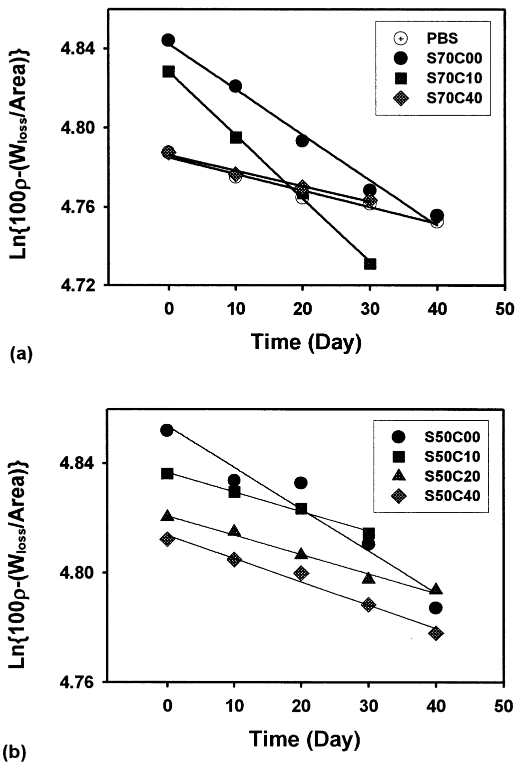

Fig. 14. Ln plots of Eq. (3)-10-iii. (a) PBS and S70 series (b) S50 series.

20 mol% feed, and it begins to rise in the sample that was fed 40 mol% CHDM. However, the *k* value does not increase so much as the hydrolytic degradation in the sample of S50C40. The reason is that the biodegradation of the polymer occurs only on the surface of the sample, which is unlike the hydrolytic degradation. Therefore the magnitude of ascending *k* value of S50C40 is not so high. By the same reason, S70C40 shows a low *k* value in that figure.

In the S70 series, the S70C20 sample was not used in evaluating the biodegradation because of the severe deformation of the samples during the composting experiment. Therefore, it is hard to investigate the ascending behavior of *k* in S70C40 that arises from the effect of the crystallinity. Moreover, the *k* value of S70C10 does not decrease. Rather than that, it increases slightly. This result is quite different from the S50 series and from the hydrolytic degradation, in which the *k* value decreased by the effect of the high contact angle. Therefore, the higher *k* value of S70C10 shows an optimum hydrophilic–hydrophobic balance where microorganisms can easily attack the polymer chain [28].

At all samples, we found stains, which are suspected to evidence that these copolyesters are degraded by the attack

Table 5
Density of PBCSTs

Sample	S50C00	S50C10	S50C20	S50C40
Density (g/cm^3)	1.28	1.26	1.24	1.23
Sample	S70C00	S70C10	S70C20	S70C40
Density (g/cm^3)	1.27	1.25	1.23	1.20

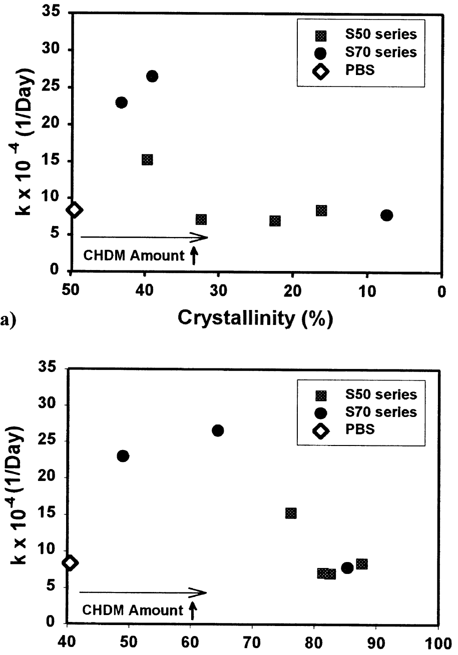

Fig. 15. Effect of the crystallinity and of the contact angle of the composting, which is evaluated with *k*. (a) Crystallinity vs. *k*. (b) Contact angle vs. *k*.

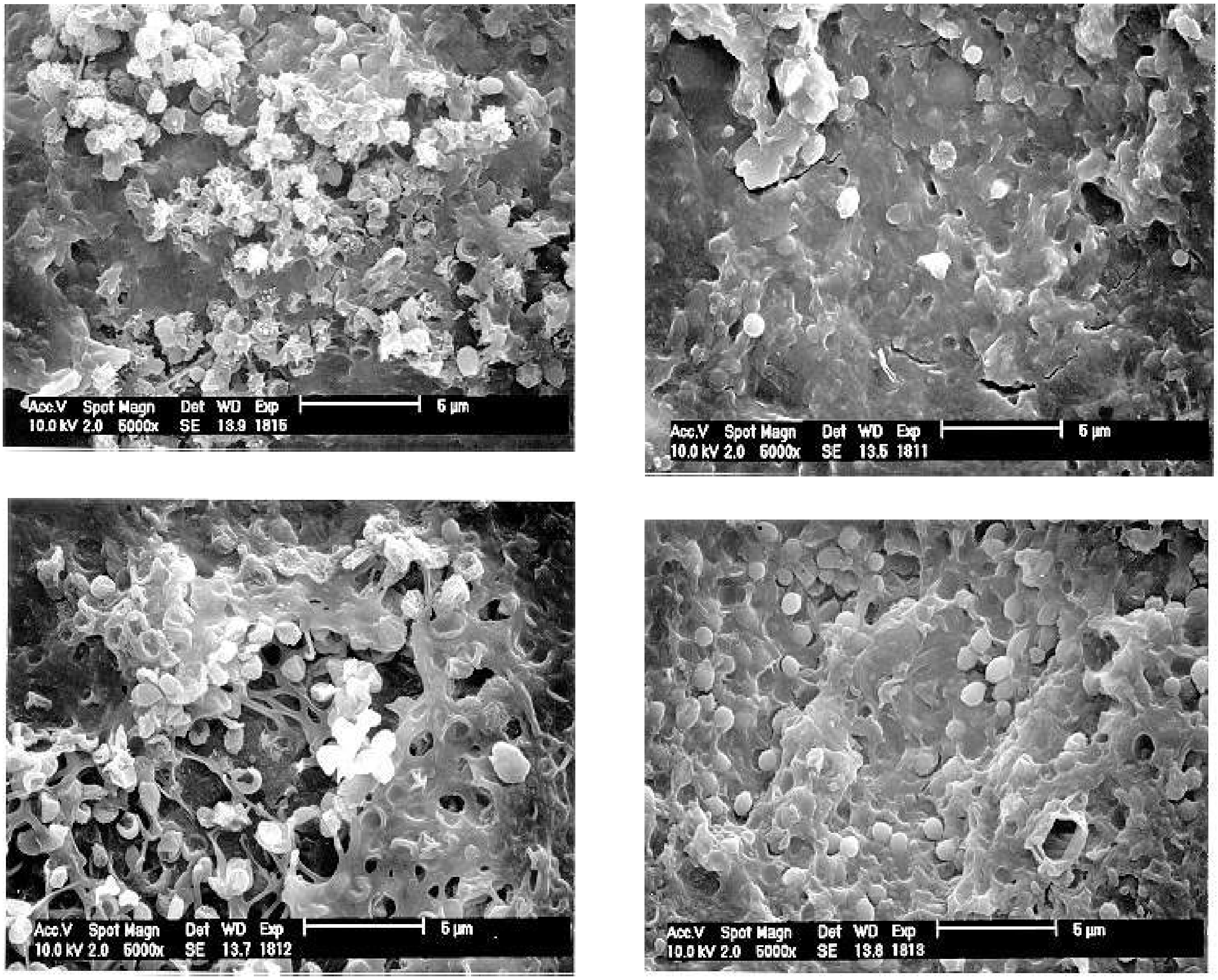

Fig. 16. Surface morphology after 40 days composting. (5000 ×, SEM).

of microorganisms. Fig. 16 shows that these stains are traces of growing microorganisms on the surface of each sample. In this figure, even in the S50C20 samples that showed the lowest weight loss, the severe surface degradation by the attack of microorganisms can be observed. These results indicate that microorganisms can attack and digest the randomly distributed aliphatic–aromatic copolyesters.

4. Conclusion

Two series of biodegradable aliphatic–aromatic random copolyesters were synthesized through the polycondensation with controlling diacid and diol parts. Their number average molecular weights were in the range of 15,000–34,000, and their decreasing behavior was observed as the composition of CHDM increased. No melting temperature in the samples, of which the feed ratio of CHDM exceeds 20%, indicated that the cyclic structure of CHDM disrupts severely the crystalline structure of those copolyesters. By ^{1}H NMR analysis, we found that the reactivity of SA and DMT is the same, and that the apparent reactivity of CHDM is better than BD. The composition and the molecular weight change with the reaction time. By these results, we confirmed that the CHDM was less extracted during the polycondensation than BD, which tendency may come from the less volatility of CHDM, which has the bulky structure. In the tensile tests, S50 series showed better properties than S70 series compared to the samples that contain the same amount of CHDM. CHDM reduced the copolyester crystallinity, and this improved the light transparency of the copolyester. Both DMT and CHDM make the copolyester surface more hydrophobic. In the hydrolytic degradation and the composting experiments, with simple degradation models, we found that not only aromatic and cyclic unit composition but also the crystallinity and the surface hydrophilicity affect the polymer biodegradation and also there is an optimum hydrophilic–hydrophobic balance in the composting biodegradation.

References

[1] Yoshie N, Azuma Y, Sakurai M, Inoue Y. J Appl Polym Sci 1995;56:17.

[2] Gonsalves KE, Chen X, Cameron JA. Macromolecules 1992;25:3309.

[3] Kim YJ, Lee HM, Lee YM, Park OO. Kor J Ch Engng 1994;11(3):172.

[4] Kim YJ, Lee HM, Park OO. Polym Engng Sci 1995;35(20):1652.

[5] Montando G, Montando MS, Scampornno E, Vitalini D. Macromolecules 1992;25:5099.

[6] Tokiwa Y, Suzoki T. J Appl Polym Sci 1981;26:441–8.

[7] Darby RT, Kaplan AM. Appl Microbiol 1968;16:900.

[8] Potts JE, Cending RA, Ackart WB, Niegisch WD. Polym Prepr (Am Chem Soc, Div Polym Chem) 1972;13:629.

[9] Encyclopedia of Polymer Sci &,Engng. Vol. 12. p. 28–36.

[10] Gu J, Coulter S, Eberiel D, McCarthy SP, Gross RA. J Environ Polym Degrad 1993;1(2):143–53.

[11] De Kesel C, Wauven CV, David C. Polym Degrad Stab 1997;55:107–13.

[12] Fuller CS, Frosch CJ. J Appl Phys 1969:31.

[13] Bloembergen S, Holden DA, Bluhm TL, Harmer GK, Marchessault RH. Macromolecules 1989;22:1663.

[14] Yoshie N, Inoue Y, Yoo HY, Okui N. Polymer 1994;35:1931.

[15] Biggs BS, Erickson RH, Fuller CS. Ind Engng Chem 1947;39:1090.

[16] Bitritto MM, Bell JP, Brenkle GM, Huang SJ, Knox JR. J Appl Polym Sci 1979;35:405–14.

[17] P JH, Fletcher M. Appl Environ Microbiol 1998;March(30):811–7.

[18] vert M, Li W. Die Angewandte Makromolekulare Chemie 1997;247:239–53.

[19] Morrison, Boyd. Organic chemistry. 6th ed.. Englewood Cliffs, NJ: Prentice-Hall, 1992.

[20] Krevelen. Properties of polymers. 3rd ed. Amsterdam: Elsevier, 1990.

[21] Zhan H, Ward IM. Macromolecules 1995;28:7622–9.

[22] Allen NS, Edge M, Mohannadian M. Eur Polym J 1991;27:1373.

[23] Li Suming. J Biomed Mater Res 1999;48(3).

[24] Fisher EW, Sterzel HJ, Wegner G. Kolloid Z Z Polym 1973;251:980.

[25] Muller RJ, Deckwer WD. J Environ Polym Degrad 1995;3:215–23.

[26] Kawai F. J Environ Polym Degrad 1996;4(1):21–8.

[27] Kleeberg I, Hetz C, Kroppenstedt RM. Appl Environ Microbiol 1998;64(5):1731–5.

[28] Kim YD. KAIST. PhD thesis, 1998. p. 65.